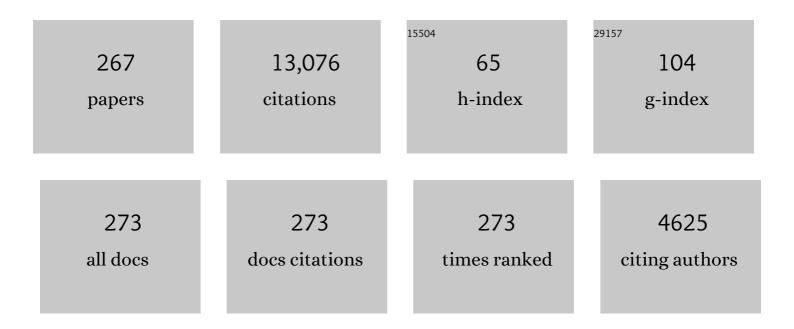
List of Publications by Year in descending order

Source: https://exaly.com/author-pdf/1244710/publications.pdf Version: 2024-02-01



PM CELLEDS

#	Article	IF	CITATIONS
1	Fuel gain exceeding unity in an inertially confined fusion implosion. Nature, 2014, 506, 343-348.	27.8	742
2	Line-imaging velocimeter for shock diagnostics at the OMEGA laser facility. Review of Scientific Instruments, 2004, 75, 4916-4929.	1.3	394
3	Polarization-Modulated Second Harmonic Generation in Collagen. Biophysical Journal, 2002, 82, 3330-3342.	0.5	375
4	Absolute Equation of State Measurements on Shocked Liquid Deuterium up to 200 GPa (2 Mbar). Physical Review Letters, 1997, 78, 483-486.	7.8	342
5	Measurements of the Equation of State of Deuterium at the Fluid Insulator-Metal Transition. , 1998, 281, 1178-1181.		326
6	Progress towards ignition on the National Ignition Facility. Physics of Plasmas, 2013, 20, .	1.9	259
7	Burning plasma achieved in inertial fusion. Nature, 2022, 601, 542-548.	27.8	233
8	Onset of Hydrodynamic Mix in High-Velocity, Highly Compressed Inertial Confinement Fusion Implosions. Physical Review Letters, 2013, 111, 085004.	7.8	215
9	Melting temperature of diamond at ultrahighÂpressure. Nature Physics, 2010, 6, 40-43.	16.7	210
10	Shock-Induced Transformation of Liquid Deuterium into a Metallic Fluid. Physical Review Letters, 2000, 84, 5564-5567.	7.8	202
11	Ramp compression of diamond to five terapascals. Nature, 2014, 511, 330-333.	27.8	195
12	Electron Density Measurements of High Density Plasmas Using Soft X-Ray Laser Interferometry. Physical Review Letters, 1995, 74, 3991-3994.	7.8	193
13	Experimental evidence for superionic water ice using shock compression. Nature Physics, 2018, 14, 297-302.	16.7	165
14	Dissociation of Liquid Silica at High Pressures and Temperatures. Physical Review Letters, 2006, 97, 025502.	7.8	158
15	Phase Transformations and Metallization of Magnesium Oxide at High Pressure and Temperature. Science, 2012, 338, 1330-1333.	12.6	156
16	The high-foot implosion campaign on the National Ignition Facility. Physics of Plasmas, 2014, 21, .	1.9	149
17	Quantitative second-harmonic generation microscopy in collagen. Applied Optics, 2003, 42, 5209.	2.1	144
18	Inertially confined fusion plasmas dominated by alpha-particle self-heating. Nature Physics, 2016, 12, 800-806.	16.7	144

#	Article	IF	CITATIONS
19	Streaked optical pyrometer system for laser-driven shock-wave experiments on OMEGA. Review of Scientific Instruments, 2007, 78, 034903.	1.3	143
20	Laser-driven single shock compression of fluid deuterium from 45 to 220 GPa. Physical Review B, 2009, 79, .	3.2	138
21	Capsule implosion optimization during the indirect-drive National Ignition Campaign. Physics of Plasmas, 2011, 18, .	1.9	131
22	Implosion dynamics measurements at the National Ignition Facility. Physics of Plasmas, 2012, 19, .	1.9	125
23	Shock compression of stishovite and melting of silica at planetary interior conditions. Science, 2015, 347, 418-420.	12.6	123
24	High-precision measurements of the equation of state of hydrocarbons at 1–10 Mbar using laser-driven shock waves. Physics of Plasmas, 2010, 17, .	1.9	119
25	High-density carbon ablator experiments on the National Ignition Facility. Physics of Plasmas, 2014, 21, .	1.9	116
26	Shock timing experiments on the National Ignition Facility: Initial results and comparison with simulation. Physics of Plasmas, 2012, 19, .	1.9	115
27	Accurate measurement of laser-driven shock trajectories with velocity interferometry. Applied Physics Letters, 1998, 73, 1320-1322.	3.3	113
28	A high-resolution integrated model of the National Ignition Campaign cryogenic layered experiments. Physics of Plasmas, 2012, 19, .	1.9	108
29	Insulator-metal transition in dense fluid deuterium. Science, 2018, 361, 677-682.	12.6	108
30	Symmetry control of an indirectly driven high-density-carbon implosion at high convergence and high velocity. Physics of Plasmas, 2017, 24, .	1.9	106
31	Achieving high-density states through shock-wave loading of precompressed samples. Proceedings of the United States of America, 2007, 104, 9172-9177.	7.1	103
32	Hugoniot Data for Helium in the Ionization Regime. Physical Review Letters, 2008, 100, 124503.	7.8	103
33	Demonstration of High Performance in Layered Deuterium-Tritium Capsule Implosions in Uranium Hohlraums at the National Ignition Facility. Physical Review Letters, 2015, 115, 055001.	7.8	101
34	Shock-Induced Transformation ofAl2O3and LiF into Semiconducting Liquids. Physical Review Letters, 2003, 91, 035502.	7.8	97
35	Electronic conduction in shock-compressed water. Physics of Plasmas, 2004, 11, L41-L44.	1.9	96
36	Coupling static and dynamic compressions: first measurements in dense hydrogen. High Pressure Research, 2004, 24, 25-31.	1.2	96

3

#	Article	IF	CITATIONS
37	Cryogenic thermonuclear fuel implosions on the National Ignition Facility. Physics of Plasmas, 2012, 19, .	1.9	95
38	Extended data set for the equation of state of warm dense hydrogen isotopes. Physical Review B, 2012, 86, .	3.2	95
39	Diamond spheres for inertial confinement fusion. Nuclear Fusion, 2009, 49, 112001.	3.5	94
40	Insulator-to-Conducting Transition in Dense Fluid Helium. Physical Review Letters, 2010, 104, 184503.	7.8	93
41	High-energy x-ray microscopy techniques for laser-fusion plasma research at the National Ignition Facility. Applied Optics, 1998, 37, 1784.	2.1	89
42	Shock compression of quartz in the high-pressure fluid regime. Physics of Plasmas, 2005, 12, 082702.	1.9	89
43	Stiff Response of Aluminum under Ultrafast Shockless Compression to 110ÂGPA. Physical Review Letters, 2007, 98, 065701.	7.8	87
44	Strength effects in diamond under shock compression from 0.1 to 1 TPa. Physical Review B, 2010, 81, .	3.2	87
45	Design of inertial fusion implosions reaching the burning plasma regime. Nature Physics, 2022, 18, 251-258.	16.7	87
46	Shock timing technique for the National Ignition Facility. Physics of Plasmas, 2001, 8, 2245-2250.	1.9	86
47	Temperature Measurements of Shock Compressed Liquid Deuterium up to 230 GPa. Physical Review Letters, 2001, 87, 165504.	7.8	86
48	High-Performance Indirect-Drive Cryogenic Implosions at High Adiabat on the National Ignition Facility. Physical Review Letters, 2018, 121, 135001.	7.8	86
49	Thermal equilibration in a shock wave. Physical Review Letters, 1992, 68, 2305-2308.	7.8	85
50	Reflectivity of intense femtosecond laser pulses from a simple metal. Physical Review Letters, 1994, 72, 3351-3354.	7.8	85
51	Absolute Equation-of-State Data in the 10–40 Mbar (1–4 TPa) Regime. Physical Review Letters, 1998, 80, 1248-1251.	7.8	85
52	Precision Shock Tuning on the National Ignition Facility. Physical Review Letters, 2012, 108, 215004.	7.8	83
53	High-precision measurements of the diamond Hugoniot in and above the melt region. Physical Review B, 2008, 78, .	3.2	82
54	Demonstration of the shock-timing technique for ignition targets on the National Ignition Facility. Physics of Plasmas, 2009, 16, .	1.9	82

#	Article	IF	CITATIONS
55	Electron-ion equilibration in a strongly coupled plasma. Physical Review E, 1995, 52, 4299-4310.	2.1	81
56	Shock Compressing Diamond to a Conducting Fluid. Physical Review Letters, 2004, 93, 195506.	7.8	81
57	Dynamic symmetry of indirectly driven inertial confinement fusion capsules on the National Ignition Facility. Physics of Plasmas, 2014, 21, .	1.9	81
58	Convergent ablator performance measurements. Physics of Plasmas, 2010, 17, .	1.9	80
59	of Plasmas, 2015, 22, 056318.	1.9	80
60	Pulse-dilation enhanced gated optical imager with 5 ps resolution (invited). Review of Scientific Instruments, 2010, 81, 10E317.	1.3	79
61	Laser-driven shock experiments on precompressed water: Implications for "icy―giant planets. Journal of Chemical Physics, 2006, 125, 014701.	3.0	77
62	The velocity campaign for ignition on NIF. Physics of Plasmas, 2012, 19, .	1.9	76
63	Systematic uncertainties in shock-wave impedance-match analysis and the high-pressure equation of state of Al. Journal of Applied Physics, 2005, 98, 113529.	2.5	75
64	Equation of State Data for Iron at Pressures beyond 10 Mbar. Physical Review Letters, 2002, 88, 235502.	7.8	73
65	Equation of state of iron under core conditions of large rocky exoplanets. Nature Astronomy, 2018, 2, 452-458.	10.1	71
66	National Ignition Facility Laser System Performance. Fusion Science and Technology, 2016, 69, 366-394.	1.1	70
67	Analysis of laser shock experiments on precompressed samples using a quartz reference and application to warm dense hydrogen and helium. Journal of Applied Physics, 2015, 118, .	2.5	69
68	Nuclear imaging of the fuel assembly in ignition experiments. Physics of Plasmas, 2013, 20, 056320.	1.9	65
69	Progress in hohlraum physics for the National Ignition Facility. Physics of Plasmas, 2014, 21, .	1.9	62
70	Cryogenic tritium-hydrogen-deuterium and deuterium-tritium layer implosions with high density carbon ablators in near-vacuum hohlraums. Physics of Plasmas, 2015, 22, 062703.	1.9	62
71	Influence of pulse duration on ultrashort laser pulse ablation of biological tissues. Journal of Biomedical Optics, 2001, 6, 332.	2.6	61
72	Evidence for a Phase Transition in Silicate Melt at Extreme Pressure and Temperature Conditions. Physical Review Letters, 2012, 108, 065701.	7.8	61

#	Article	IF	CITATIONS
73	Development of Improved Radiation Drive Environment for High Foot Implosions at the National Ignition Facility. Physical Review Letters, 2016, 117, 225002.	7.8	61
74	Compression Freezing Kinetics of Water to Ice VII. Physical Review Letters, 2017, 119, 025701.	7.8	60
75	Integrated modeling of cryogenic layered highfoot experiments at the NIF. Physics of Plasmas, 2016, 23, .	1.9	59
76	Absolute measurements of the equations of state of low-Z materials in the multi-Mbar regime using laser-driven shocks. Physics of Plasmas, 1997, 4, 1857-1861.	1.9	58
77	Properties of fluid deuterium under double-shock compression to several Mbar. Physics of Plasmas, 2004, 11, L49-L52.	1.9	58
78	Refractive index of lithium fluoride ramp compressed to 800 GPa. Journal of Applied Physics, 2011, 109, .	2.5	58
79	Assembly of High-Areal-Density Deuterium-Tritium Fuel from Indirectly Driven Cryogenic Implosions. Physical Review Letters, 2012, 108, 215005.	7.8	57
80	Equation of state of CH <mml:math <br="" xmlns:mml="http://www.w3.org/1998/Math/MathML">display="inline"&gt;<mml:msub><mml:mrow /&gt;<mml:mrow><mml:mn>1.36</mml:mn></mml:mrow></mml:mrow </mml:msub></mml:math> : First-principles molecular dynamics simulations and shock-and-release wave speed measurements. Physical Review B,	3.2	57
81	2012, 86, . Thin Shell, High Velocity Inertial Confinement Fusion Implosions on the National Ignition Facility. Physical Review Letters, 2015, 114, 145004.	7.8	56
82	Electrical Conductivity of a Dense Plasma. Physical Review Letters, 1986, 57, 1595-1598.	7.8	55
83	Velocity and Timing of Multiple Spherically Converging Shock Waves in Liquid Deuterium. Physical Review Letters, 2011, 106, 195005.	7.8	54
84	A Review of Equation-of-State Models for Inertial Confinement Fusion Materials. High Energy Density Physics, 2018, 28, 7-24.	1.5	54
85	A high-resolution two-dimensional imaging velocimeter. Review of Scientific Instruments, 2010, 81, 035101.	1.3	51
86	Capsule performance optimization in the National Ignition Campaign. Physics of Plasmas, 2010, 17, .	1.9	51
87	The near vacuum hohlraum campaign at the NIF: A new approach. Physics of Plasmas, 2016, 23, .	1.9	51
88	Optical probing of hot expanded states produced by shock release. Physical Review E, 1993, 47, 3547-3565.	2.1	49
89	Electron density measurement of a colliding plasma using soft-x-ray laser interferometry. Physical Review E, 1997, 55, 6293-6296.	2.1	49
90	Ramp compression of iron to 273 GPa. Journal of Applied Physics, 2013, 114, .	2.5	49

#	Article	IF	CITATIONS
91	The role of hot spot mix in the low-foot and high-foot implosions on the NIF. Physics of Plasmas, 2017, 24, .	1.9	49
92	Performance of High-Convergence, Layered DT Implosions with Extended-Duration Pulses at the National Ignition Facility. Physical Review Letters, 2013, 111, 215001.	7.8	47
93	Ablation scaling in steadyâ€state ablation dominated by inverseâ€bremsstrahlung absorption. Applied Physics Letters, 1984, 45, 1046-1048.	3.3	45
94	Direct Measurement of Energetic Electrons Coupling to an Imploding Low-Adiabat Inertial Confinement Fusion Capsule. Physical Review Letters, 2012, 108, 135006.	7.8	44
95	The direct measurement of ablation pressure driven by 351-nm laser radiation. Journal of Applied Physics, 2011, 110, .	2.5	43
96	Micron-Resolution Radiography of Laser-Accelerated and X-Ray Heated Foils with an X-Ray Laser. Physical Review Letters, 1995, 74, 3816-3819.	7.8	42
97	Equation of state measurements of hydrogen isotopes on Nova. Physics of Plasmas, 1998, 5, 1864-1869.	1.9	42
98	Evidence of hydrogenâ^'helium immiscibility at Jupiter-interior conditions. Nature, 2021, 593, 517-521.	27.8	41
99	The effect of laser pulse shape variations on the adiabat of NIF capsule implosions. Physics of Plasmas, 2013, 20, .	1.9	40
100	Spatial filter pinhole for high-energy pulsed lasers. Applied Optics, 1998, 37, 2371.	2.1	39
101	Measurement of localized heating in the focus of an optical trap. Applied Optics, 2000, 39, 3396.	2.1	39
102	Progress in the indirect-drive National Ignition Campaign. Plasma Physics and Controlled Fusion, 2012, 54, 124026.	2.1	38
103	High-density carbon capsule experiments on the national ignition facility. Physical Review E, 2015, 91, 021101.	2.1	38
104	Performance of indirectly driven capsule implosions on the National Ignition Facility using adiabat-shaping. Physics of Plasmas, 2016, 23, 056303.	1.9	38
105	First beryllium capsule implosions on the National Ignition Facility. Physics of Plasmas, 2016, 23, 056310.	1.9	37
106	Measurement of Body-Centered-Cubic Aluminum at 475ÂGPa. Physical Review Letters, 2017, 119, 175702.	7.8	37
107	Conversion of laser light into x rays in thin foil targets. Physical Review A, 1990, 41, 3270-3280.	2.5	35
108	Progress towards ignition on the National Ignition Facility. Nuclear Fusion, 2011, 51, 094024.	3.5	35

#	Article	IF	CITATIONS
109	Multiple spherically converging shock waves in liquid deuterium. Physics of Plasmas, 2011, 18, 092706.	1.9	34
110	Absolute calibration of the OMEGA streaked optical pyrometer for temperature measurements of compressed materials. Review of Scientific Instruments, 2016, 87, 114903.	1.3	34
111	Fringe formation and coherence of a soft-x-ray laser beam illuminating a Mach–Zehnder interferometer. Optics Letters, 1995, 20, 1907.	3.3	33
112	Symmetry tuning of a near one-dimensional 2-shock platform for code validation at the National Ignition Facility. Physics of Plasmas, 2016, 23, .	1.9	33
113	Hugoniot and release measurements in diamond shocked up to 26 Mbar. Physical Review B, 2017, 95, .	3.2	32
114	Probing the seeding of hydrodynamic instabilities from nonuniformities in ablator materials using 2D velocimetry. Physics of Plasmas, 2018, 25, .	1.9	32
115	Shock-timing experiments using double-pulse laser irradiation. Physics of Plasmas, 2006, 13, 056303.	1.9	31
116	Adiabat-shaping in indirect drive inertial confinement fusion. Physics of Plasmas, 2015, 22, 052702.	1.9	31
117	Examining the radiation drive asymmetries present in the high foot series of implosion experiments at the National Ignition Facility. Physics of Plasmas, 2017, 24, .	1.9	31
118	Review of hydrodynamic instability experiments in inertially confined fusion implosions on National Ignition Facility. Plasma Physics and Controlled Fusion, 2020, 62, 014007.	2.1	31
119	Heat front propagation in femtosecond-laser-heated solids. Physical Review E, 1995, 51, R5208-R5211.	2.1	30
120	High pressures generated by laser driven shocks: applications to planetary physics. Nuclear Fusion, 2004, 44, S208-S214.	3.5	30
121	Optimization of xâ€ray sources for proximity lithography produced by a high average power Nd:glass laser. Journal of Applied Physics, 1996, 79, 8258-8268.	2.5	29
122	X-ray preheating of window materials in direct-drive shock-wave timing experiments. Physics of Plasmas, 2006, 13, 122702.	1.9	29
123	First results of radiation-driven, layered deuterium-tritium implosions with a 3-shock adiabat-shaped drive at the National Ignition Facility. Physics of Plasmas, 2015, 22, .	1.9	29
124	Measurement of High-Pressure Shock Waves in Cryogenic Deuterium-Tritium Ice Layered Capsule Implosions on NIF. Physical Review Letters, 2013, 111, 065003.	7.8	28
125	Thermodynamic properties of <mml:math xmlns:mml="http://www.w3.org/1998/Math/MathML"&gt; <mml:mi>MgSiO</mml:mi> <mml:msub> <mml:mrow /&gt; <mml:mn>3</mml:mn> </mml:mrow </mml:msub>  at super-Earth mantle conditions. Physical Review B, 2018. 97</mml:math 	3.2	28
126	High planarity x-ray drive for ultrafast shockless-compression experiments. Physics of Plasmas, 2007, 14, 057105.	1.9	27

#	Article	IF	CITATIONS
127	Streaked radiography measurements of convergent ablator performance (invited). Review of Scientific Instruments, 2010, 81, 10E304.	1.3	27
128	Shock timing measurements and analysis in deuterium-tritium-ice layered capsule implosions on NIF. Physics of Plasmas, 2014, 21, 022703.	1.9	27
129	X-ray scattering measurements of dissociation-induced metallization of dynamically compressed deuterium. Nature Communications, 2016, 7, 11189.	12.8	27
130	Experimental results of radiation-driven, layered deuterium-tritium implosions with adiabat-shaped drives at the National Ignition Facility. Physics of Plasmas, 2016, 23, .	1.9	27
131	Equation of State and Material Property Measurements of Hydrogen Isotopes at the Highâ€Pressure, Highâ€Temperature Insulatorâ€Metal Transition. Astrophysical Journal, Supplement Series, 2000, 127, 267-273.	7.7	26
132	Shock-wave equation-of-state measurements in fused silica up to 1600 GPa. Journal of Applied Physics, 2016, 119, .	2.5	26
133	Shock Compression of Liquid Deuterium up to 1ÂTPa. Physical Review Letters, 2019, 122, 255702.	7.8	26
134	Hotspot parameter scaling with velocity and yield for high-adiabat layered implosions at the National Ignition Facility. Physical Review E, 2020, 102, 023210.	2.1	25
135	Yield and compression trends and reproducibility at NIF*. High Energy Density Physics, 2020, 36, 100755.	1.5	25
136	Experimental validation of a diagnostic technique for tuning the fourth shock timing on National Ignition Facility. Physics of Plasmas, 2010, 17, 012703.	1.9	24
137	Two-dimensional imaging velocity interferometry: Data analysis techniques. Review of Scientific Instruments, 2012, 83, 043116.	1.3	24
138	Early time implosion symmetry from two-axis shock-timing measurements on indirect drive NIF experiments. Physics of Plasmas, 2014, 21, .	1.9	24
139	Equation of state, adiabatic sound speed, and Grüneisen coefficient of boron carbide along the principal Hugoniot to 700 GPa. Physical Review B, 2016, 94, .	3.2	24
140	Heterogeneous flow and brittle failure in shock-compressed silicon. Journal of Applied Physics, 2013, 114, .	2.5	23
141	Progress toward ignition at the National Ignition Facility. Plasma Physics and Controlled Fusion, 2013, 55, 124015.	2.1	23
142	Hugoniot experiments with unsteady waves. Journal of Applied Physics, 2014, 116, .	2.5	23
143	Theoretical and experimental investigation of the equation of state of boron plasmas. Physical Review E, 2018, 98, 023205.	2.1	23
144	Mix and hydrodynamic instabilities on NIF. Journal of Instrumentation, 2017, 12, C06001-C06001.	1.2	21

#	Article	IF	CITATIONS
145	Measuring the shock impedance mismatch between high-density carbon and deuterium at the National Ignition Facility. Physical Review B, 2018, 97, .	3.2	21
146	Achieving 280 Gbar hot spot pressure in DT-layered CH capsule implosions at the National Ignition Facility. Physics of Plasmas, 2020, 27, .	1.9	20
147	Application of cross-beam energy transfer to control drive symmetry in ICF implosions in low gas fill <i>Hohlraums</i> at the National Ignition Facility. Physics of Plasmas, 2020, 27, .	1.9	18
148	X-ray diffraction of ramp-compressed aluminum to 475 GPa. Physics of Plasmas, 2018, 25, .	1.9	17
149	Hugoniot, sound velocity, and shock temperature of MgO to 2300ÂGPa. Physical Review B, 2019, 100, .	3.2	17
150	Constraining computational modeling of indirect drive double shell capsule implosions using experiments. Physics of Plasmas, 2021, 28, .	1.9	17
151	Simultaneous Measurement of Local Gain and Electron Density in X-ray Lasers. Science, 1996, 273, 1093-1096.	12.6	16
152	Implosion shape control of high-velocity, large case-to-capsule ratio beryllium ablators at the National Ignition Facility. Physics of Plasmas, 2018, 25, 072708.	1.9	16
153	Equation of State of <mml:math <br="" xmlns:mml="http://www.w3.org/1998/Math/MathML">display="inline"&gt;<mml:mrow><mml:msub><mml:mrow><mml:mi>CO</mml:mi></mml:mrow><ml:mrow><n Shock Compressed to 1ÂTPa. Physical Review Letters, 2020, 125, 165701.</n </ml:mrow></mml:msub></mml:mrow></mml:math>	າml <b>:ກາຍ</b> >2<	/mmb&mn>
154	Xâ€ray lasers for high density plasma diagnostics (invited). Review of Scientific Instruments, 1995, 66, 574-578.	1.3	15
155	Extreme-ultraviolet interferometry at 155 nm using multilayer optics. Applied Optics, 1995, 34, 6389.	2.1	15
156	A simulation-based and analytic analysis of the off-Hugoniot response of alternative inertial confinement fusion ablator materials. High Energy Density Physics, 2016, 20, 23-28.	1.5	15
157	Direct-drive measurements of laser-imprint-induced shock velocity nonuniformities. Physical Review E, 2019, 99, 063208.	2.1	15
158	Developing quartz and molybdenum as impedance-matching standards in the 100-Mbar regime. Physical Review B, 2019, 99, .	3.2	15
159	Imaging VISAR diagnostic for the National Ignition Facility (NIF). , 2005, , .		14
160	Measurements of the sound velocity of shock-compressed liquid silica to 1100 GPa. Journal of Applied Physics, 2016, 120, .	2.5	14
161	Performance of beryllium targets with full-scale capsules in low-fill 6.72-mm hohlraums on the National Ignition Facility. Physics of Plasmas, 2017, 24, .	1.9	14
162	Dynamics of laser-driven shock waves in fused silica. Physical Review Letters, 1987, 58, 214-217.	7.8	13

#	Article	IF	CITATIONS
163	Experimental studies of ICF indirect-drive Be and high density C candidate ablators. Journal of Physics: Conference Series, 2008, 112, 022004.	0.4	13
164	Equations of State for Ablator Materials in Inertial Confinement Fusion Simulations. Journal of Physics: Conference Series, 2016, 717, 012082.	0.4	13
165	Nondestructive single-shot soft x-ray lithography and contact microscopy using a laser-produced plasma source. Applied Optics, 1987, 26, 4313.	2.1	12
166	Application of x-ray-laser interferometry to study high-density laser-produced plasmas. Journal of the Optical Society of America B: Optical Physics, 1996, 13, 447.	2.1	12
167	Comparison of soft and hard tissue ablation with sub-ps and ns pulse lasers. , 1996, , .		12
168	<title>Imaging collagen orientation using polarization-modulated second harmonic generation</title> . , 2002, , .		12
169	Deficiencies in compression and yield in x-ray-driven implosions. Physics of Plasmas, 2020, 27, .	1.9	12
170	The first target experiments on the National Ignition Facility. European Physical Journal D, 2007, 44, 273-281.	1.3	11
171	Quasi-isentropic material property studies at extreme pressures: from omega to NIF. Journal of Physics: Conference Series, 2008, 112, 042024.	0.4	11
172	Shock equation of state of <mml:math xmlns:mml="http://www.w3.org/1998/Math/MathML"&gt; <mml:mmultiscripts> <mml:mi>LiH</mml:mi> <mml:mprese /&gt; <mml:none></mml:none> <mml:mn>6</mml:mn> </mml:mprese </mml:mmultiscripts>  to 1.1 TPa. Physical Review B, 2017, 96, .</mml:math 	cripts 3.2	11
173	Fuel convergence sensitivity in indirect drive implosions. Physics of Plasmas, 2021, 28, 042705.	1.9	11
174	Experiments to explore the influence of pulse shaping at the National Ignition Facility. Physics of Plasmas, 2020, 27, 112708.	1.9	11
175	Two-dimensional rarefaction of laser-irradiated thin foils. Physics of Fluids, 1984, 27, 2774.	1.4	10
176	Simultaneous multi-element determination using helium or argon plasma for graphite furnace capacitively coupled plasma atomic emission spectrometry. Journal of Analytical Atomic Spectrometry, 1993, 8, 809.	3.0	10
177	Experiments Using Laser-driven Shockwaves for EOS and Transport Measurements. Contributions To Plasma Physics, 2001, 41, 239-242.	1.1	10
178	Hydrodynamic instability seeding by oxygen nonuniformities in glow discharge polymer inertial fusion ablators. Physical Review E, 2018, 98, .	2.1	10
179	Measurement of the sound speed in dense fluid deuterium along the cryogenic liquid Hugoniot. Physics of Plasmas, 2019, 26, .	1.9	10
180	Reflectivity of a shocked solid surface. Optics Communications, 1986, 56, 425-429.	2.1	9

#	Article	IF	CITATIONS
181	Equation of state of water in the megabar range. Laser and Particle Beams, 2001, 19, 111-115.	1.0	9
182	Fielding of an imaging VISAR diagnostic at the National Ignition Facility (NIF). , 2004, 5523, 148.		9
183	Measurement of the sound velocity and Grüneisen parameter of polystyrene at inertial confinement fusion conditions. Physical Review B, 2020, 102, .	3.2	9
184	Interferometric measurements of refractive index and dispersion at high pressure. Scientific Reports, 2021, 11, 5610.	3.3	9
185	Temperature Feedback and Collagen Cross-Linking in Argon Laser Vascular Welding. Lasers in Medical Science, 1998, 13, 98-105.	2.1	8
186	Two-color mid-infrared thermometer with a hollow glass optical fiber. Applied Optics, 1998, 37, 6677.	2.1	8
187	Shockâ€Compression Experiments and Reflectivity Measurements in Deuterium up to 3.5 Mbar using the Nova Laser. Contributions To Plasma Physics, 1999, 39, 13-16.	1.1	8
188	Hard x-ray (>100 keV) imager to measure hot electron preheat for indirectly driven capsule implosions on the NIF. Review of Scientific Instruments, 2012, 83, 10E508.	1.3	8
189	Recent and planned hydrodynamic instability experiments on indirect-drive implosions on the National Ignition Facility. High Energy Density Physics, 2020, 36, 100820.	1.5	8
190	Laser-driven shock wave experiments at the University of British Columbia. Laser and Particle Beams, 1986, 4, 555-567.	1.0	7
191	Experimental and Computational Laser Tissue Welding Using a Protein Patch. Journal of Biomedical Optics, 1998, 3, 96.	2.6	7
192	Chost fringe removal techniques using Lissajous data presentation. Review of Scientific Instruments, 2016, 87, 033106.	1.3	7
193	High-precision shock equation of state measurements for metallic fluid carbon between 15 and 20 Mbar. Physics of Plasmas, 2020, 27, .	1.9	7
194	Principal factors in performance of indirect-drive laser fusion experiments. Physics of Plasmas, 2020, 27, .	1.9	7
195	Overview of the line-imaging VISAR diagnostic at the National Ignition Facility (NIF). , 2007, , .		7
196	Mechanisms of shape transfer and preheating in indirect-drive double shell collisions. Physics of Plasmas, 2022, 29, .	1.9	7
197	Evidence for Dissociation and Ionization in Shock Compressed Nitrogen to 800ÂGPa. Physical Review Letters, 2022, 129, .	7.8	7
198	Effect of structural modification on second harmonic generation in collagen. , 2003, , .		6

#	Article	IF	CITATIONS
199	The effect of condensates and inner coatings on the performance of vacuum hohlraum targets. Physics of Plasmas, 2010, 17, 032701.	1.9	6
200	Using a 2-shock 1D platform at NIF to measure the effect of convergence on mix and symmetry. Physics of Plasmas, 2018, 25, 102702.	1.9	6
201	Breakdown of Fermi Degeneracy in the Simplest Liquid Metal. Physical Review Letters, 2019, 122, 085001.	7.8	6
202	Benchmarking boron carbide equation of state using computation and experiment. Physical Review E, 2020, 102, 053203.	2.1	6
203	Dynamic compression of water to conditions in ice giant interiors. Scientific Reports, 2022, 12, 715.	3.3	6
204	Combining a thermal-imaging diagnostic with an existing imaging VISAR diagnostic at the National Ignition Facility (NIF). , 2005, , .		5
205	Shock Experiments on Pre-Compressed Fluid Helium. , 2009, , .		5
206	Response to Comment on "Insulator-metal transition in dense fluid deuterium― Science, 2019, 363, .	12.6	5
207	Optimization of capsule dopant levels to improve fuel areal density*. High Energy Density Physics, 2020, 37, 100884.	1.5	5
208	Equation-of-state, sound speed, and reshock of shock-compressed fluid carbon dioxide. Physics of Plasmas, 2021, 28, .	1.9	5
209	<title>Two-color infrared thermometer for low-temperature measurement using a hollow glass optical fiber</title> ., 1997, 2977, 115.		4
210	Laser-shock-driven laboratory measurements of the equation of state of hydrogen isotopes in the megabar regime. High Pressure Research, 2000, 16, 281-290.	1.2	4
211	MEASUREMENTS OF THE RELEASE OF ALPHA QUARTZ: A NEW STANDARD FOR IMPEDANCE-MATCHING EXPERIMENTS. AIP Conference Proceedings, 2008, , .	0.4	4
212	Holographic and time-resolving ability of pulse-pair two-dimensional velocity interferometry. Review of Scientific Instruments, 2014, 85, 063115.	1.3	4
213	NIF Rugby High Foot Campaign from the design side. Journal of Physics: Conference Series, 2016, 717, 012035.	0.4	4
214	Off-Hugoniot characterization of alternative inertial confinement fusion ablator materials Journal of Physics: Conference Series, 2016, 717, 012038.	0.4	4
215	Hydroscaling indirect-drive implosions on the National Ignition Facility. Physics of Plasmas, 2022, 29, .	1.9	4
216	Two-dimensional interferogram of an exploding selenium foil using a soft X-ray laser interferometer. IEEE Transactions on Plasma Science, 1996, 24, 31-32.	1.3	3

#	Article	IF	CITATIONS
217	Interferometric and Chirped Optical Probe Techniques for Highâ€Pressure Equationâ€ofâ€State Measurements. Astrophysical Journal, Supplement Series, 2000, 127, 333-337.	7.7	3
218	Design of a streaked radiography instrument for ICF ablator tuning measurements. Review of Scientific Instruments, 2008, 79, 10E913.	1.3	3
219	Two-dimensional imaging velocity interferometry: Technique and data analysis. AIP Conference Proceedings, 2012, , .	0.4	3
220	Operational experience with optical streak cameras at the National Ignition Facility. Proceedings of SPIE, 2013, , .	0.8	3
221	Numerical refocusing of 2d-VISAR data. Journal of Physics: Conference Series, 2014, 500, 142013.	0.4	3
222	A robust in-situ warp-correction algorithm for VISAR streak camera data at the National Ignition Facility. Proceedings of SPIE, 2015, , .	0.8	3
223	Hydrodynamic instabilities and mix studies on NIF: predictions, observations, and a path forward. Journal of Physics: Conference Series, 2016, 688, 012090.	0.4	3
224	X-ray drive of beryllium capsule implosions at the National Ignition Facility. Journal of Physics: Conference Series, 2016, 717, 012058.	0.4	3
225	Techniques for studying materials under extreme states of high energy density compression. Physics of Plasmas, 2021, 28, 060901.	1.9	3
226	Single shot soft x-ray microscopy using plasmas generated by a laboratory sized Nd-glass laser. Journal of Microscopy, 1985, 140, RP1-RP2.	1.8	2
227	In-vivo argon laser vascular welding using thermal feedback: open- and closed-loop patency and collagen crosslinking. , 1997, , .		2
228	<title>XUV laser grid image refractometry applied in laser hole boring experiments</title> . , 1997, 3156, 146.		2
229	<title>Simulation studies of vapor bubble generation by short-pulse lasers</title> . , 1998, , .		2
230	A soft X-ray laser interferogram of a high-density colliding plasma. IEEE Transactions on Plasma Science, 1999, 27, 120-121.	1.3	2
231	Hohlraum designs for high velocity implosions on NIF. EPJ Web of Conferences, 2013, 59, 02002.	0.3	2
232	Upgrades to the VISAR-streaked optical pyrometer (SOP) system on NIF. Proceedings of SPIE, 2015, , .	0.8	2
233	Gated photocathode design for the P510 electron tube used in the National Ignition Facility (NIF) optical streak cameras. Proceedings of SPIE, 2015, , .	0.8	2
234	Advances in shock timing experiments on the National Ignition Facility. Journal of Physics: Conference Series, 2016, 688, 012092.	0.4	2

#	Article	IF	CITATIONS
235	Converting existing optical detectors into fast x-ray detectors. Review of Scientific Instruments, 2021, 92, 073507.	1.3	2
236	Anomalous laser penetration depths in multilayer planar targets. Applied Physics Letters, 1984, 44, 713-715.	3.3	1
237	Biological specimens imaged by soft xâ€ray contact microscopy using a plasma source produced with a laboratory sized laser. Journal of Microscopy, 1986, 144, RP5.	1.8	1
238	Role of thermal conduction in the expansion of a plasma from a vacuum interface. Canadian Journal of Physics, 1988, 66, 662-673.	1.1	1
239	High density plasma diagnostics utilizing a neon-like yttrium x-ray laser. Journal of Quantitative Spectroscopy and Radiative Transfer, 1995, 54, 97-103.	2.3	1
240	<title>Probing high-density plasmas with soft x-ray lasers</title> . , 1997, 3156, 135.		1
241	Optical alignment techniques for line-imaging velocity interferometry and line-imaging self-emission of targets at the National Ignition Facility (NIF). , 2007, , .		1
242	Ignition tuning for the National Ignition Campaign. EPJ Web of Conferences, 2013, 59, 01003.	0.3	1
243	Shock timing on the National Ignition Facility: First experiments. EPJ Web of Conferences, 2013, 59, 02004.	0.3	1
244	Shock timing on the National Ignition Facility: The first precision tuning series. EPJ Web of Conferences, 2013, 59, 02005.	0.3	1
245	Ghost fringe removal techniques using Lissajous data presentation. AIP Conference Proceedings, 2017,	0.4	1
246	The first experiments on the national ignition facility. European Physical Journal Special Topics, 2006, 133, 43-45.	0.2	1
247	Hohlraum X-ray deposition in indirect-drive ICF ablator materials. European Physical Journal Special Topics, 2006, 133, 179-181.	0.2	1
248	Overview of the line-imaging VISAR Diagnostic at the National Ignition Facility (NIF). , 2006, , .		1
249	Shock Multiplication In Multilayered Targets. , 1988, 0913, 82.		0
250	Characterization and modeling of soft X-ray lasers. , 0, , .		0
251	<title>Characterization techniques for x-ray lithography sources</title> . , 1996, , .		0
252	Dynamics of a multipleâ€pulseâ€driven xâ€ray laser plasma. Physics of Plasmas, 1996, 3, 606-613.	1.9	0

#	Article	IF	CITATIONS
253	<title>Soft x-ray laser-based moire deflectometry of dense plasmas</title> . , 1997, , .		0
254	Interferometric technique to measure shock-induced surface velocities in tissues for the determination of dynamic mechanical properties. , 1998, , .		0
255	Absolute Equation of State Measurements of Low-Z Materials at Multi-Mbar Pressures Review of High Pressure Science and Technology/Koatsuryoku No Kagaku To Gijutsu, 1998, 7, 885-887.	0.0	0
256	<title>Preliminary results on the EOS of water in the megabar range</title> . , 2001, , .		0
257	Recreating planetary cores in the laboratory. , 0, , .		0
258	Recreating core states of giant planets in the laboratory. , 2009, , .		0
259	Progress in direct-drive inertial confinement fusion. EPJ Web of Conferences, 2013, 59, 01004.	0.3	0
260	Hohlraum glint and laser pre-pulse detector for NIF experiments using velocity interferometer system for any reflector. Review of Scientific Instruments, 2014, 85, 11E608.	1.3	0
261	Performance of indirectly driven capsule implosions on NIF using adiabat-shaping. Journal of Physics: Conference Series, 2016, 717, 012045.	0.4	0
262	Equation of State Measurements at Extreme Pressures Using Laser-Driven Shocks. , 2000, , 41-50.		0
263	Laser driven quasi-isentropic compression experiments (ICE) for dynamically loading materials at high strain rates. European Physical Journal Special Topics, 2006, 134, 529-534.	0.2	0
264	Line-imaging Velocimetry for Shock Diagnostics (VISAR*). , 2013, , .		0
265	Holographic Behavior in Ultrashort Pulse-pair 2d-Velocimetry. , 2014, , .		0
266	Toward a 3D Velocity Interferometer Testbed: Early Results. , 2021, , .		0
267	Toward a 3D Velocity Interferometer Testbed: Concept and Algorithm Exploration. , 2021, , .		0